Improved Performance of Dynamic Random Access Memory

Manjulata Sahoo

Department of Computer Science and Engineering
National Institute of Technology Rourkela
Rourkela – 769 008, India

Improved Performance of Dynamic Random Access Memory

Dissertation submitted in

May 2014

to the department of

Computer Science and Engineering

of

National Institute of Technology Rourkela

in partial fulfillment of the requirements

for the degree of

Master of Technology

by

Manjulata Sahoo

(Roll 212CS1468)

under the supervision of

Dr. Ratnakar Dash

Department of Computer Science and Engineering

National Institute of Technology Rourkela

Rourkela – 769 008, India

I dedicate this thesis to my family, my husband and my son for their constant support and unconditional love. I love you all dearly....

Computer Science and Engineering
National Institute of Technology Rourkela
Rourkela-769 008, India. www.nitrkl.ac.in

Dr. Ratnakar Dash
Asst. Professor

May , 2014

Certificate

This is to certify that the work in the thesis entitled *Improved Performance of Dynamic Random Access Memory* by *Manjulata Sahoo*, bearing roll number 212CS1468, is a record of research work carried out by her under my supervision and guidance in partial fulfillment of the requirements for the award of the degree of *Master of Technology* in *Computer Science and Engineering*.

Ratnakar Dash

Author's Declaration

I, Manjulata Sahoo (Roll No.212CS1468) understand that plagiarism is defined as any one or the combination of the following

1. Uncredited verbatim copying of individual sentences, paragraphs or illustrations (such as graphs, diagrams, etc.) from any source, published or unpublished, including the internet.

2. Uncredited improper paraphrasing of pages or paragraphs (changing a few words or phrases, or rearranging the original sentence order).

3. Credited verbatim copying of a major portion of a paper (or thesis chapter) without clear delineation of who did or wrote what. (Source: IEEE, the Institute, Dec. 2004)

I have made sure that all the ideas, expressions, graphs, diagrams, etc., that are not a result of my work, are properly credited. Long phrases or sentences that had to be used verbatim from published literature have been clearly identified using quotation marks.

I affirm that no portion of my work can be considered as plagiarism and I take full responsibility if such a complaint occurs. I understand fully well that the guide of the thesis may not be in a position to check for the possibility of such incidences of plagiarism in this body of work.

Manjulata Sahoo
Master of Technology
in Computer Science
N.I.T.,Rourkela

Date:

Acknowledgement

This dissertation, though an individual work, has benefited in various ways from several people. Whilst it would be simple to name them all, it would not be easy to thank them enough.

The enthusiastic guidance and support of *Asst. Prof. Ratnakar Dash* inspired me to stretch beyond my limits. His profound insight has guided my thinking to improve the final product. My solemnest gratefulness to him.

I am also grateful to *Prof. Banshidhar Majhi* for his ceaseless support throughout my research work. My sincere thanks to *Prof. Santanu Kumar Rath* for his continuous encouragement and invaluable advice.

It is indeed a privilege to be associated with people like *Prof. B. D. Sahoo*, *Prof. D. P. Mohapatra*, *Prof. S. K. Jena*, *Prof. A. K. Turuk*, *Prof. S. Chinara*, *Prof. R. K. Mohapatra* and *Prof. M. N. Sahoo*. They have made available their support in a number of ways.

Many thanks to my comrades and fellow research colleagues. It gives me a sense of happiness to be with you all. Special thanks to *Jyoti, Sumana, Pallavi, Preena, Astha, Basanti, Ansuman, Rajkamal, Amar, Rajesh, Manish, Priyesh, Vijay* whose support gave a new breath to my research.

Finally, my heartfelt thanks to my mother for her unconditional love and sacrifice. Words fail me to express my gratitude to my beloved parents and brother who sacrificed their comfort for my betterment. My heartfelt thanks to my husband and to my son for their unconditional love, support and for everything.

Manjulata Sahoo

Abstract

Dynamic Random Access Memory (DRAM) will lose its contents due to the leakage current of the capacitor present in it. Charge retention capacity of DRAM is affected by leakage current.The temperature dependent current-voltage (I-V) characteristics of $Ba_{0.8}Sr_{0.2}TiO_3$ (BST) thin-film capacitors with and without ZrO_2 layer were studied in the temperature range of 400 to 450 K. It is observed that the leakage current is reduced for capacitors with ZrO_2 layer compared to those without this layer. The leakage current is dominated by Ohmic conduction mechanism in the low field region whereas space charge limited current (SCLC) mechanism contributes to the leakage current in the medium field region for both films. The activation energy (E_a) for Ohmic conduction process is 0.5 eV for BST films and 0.56 eV for BST/ZrO_2 multilayered film. The leakage current density is reduced by an order of magnitude for BST/ZrO_2 multilayered films compared to that of BST films in the whole electric field range. The estimated trap density (N_t) decreases from 5.1 x 10^{18} to 2.2 x 10^{18} cm^{-3} with the insertion of ZrO_2 layer. The observed reduced leakage current for capacitor with BST/ZrO_2 multilayer dielectric is due to the increase in the activation energy and decrease in the trap density and hence suitable for increasing the retention capacity of DRAM. Simulated leakage current density (J) versus electric field (E) is calculated for BST thin film capacitor at different temperatures and is compared with the experimental data. It is observed that the measured leakage current density is higher in comparison to simulated current density and is due to the effect of electrodes and dielectric thin film structure in a real capacitor.

***Keywords*:** DRAM, high dielectric constant,retention capacity, leakage current

Contents

List of Figures

List of Tables

Chapter 1

Introduction

Recently, Dynamic Random Access Memory (DRAM) is the dominant solid-state memory device in the whole microprocessor system. DRAM will lose its contents due to the leakage current of the capacitor present in it. Now-a-days, high-k materials play an important role in microelectronic devices such as capacitors and memory devices [1]. Ferroelectric barium strontium titanate [$Ba_xSr_{1-x}TiO_3$, (BST)] thin film has attracted much attention for its potential applications in devices such as dynamic random access memories (DRAM), field effect transistors (FET) because of its high dielectric constant, low leakage current, and high breakdown field [2–4]. The leakage current of the BST thin film is one of the most important issues in estimating the charge retention capacity of the capacitor [4]. Also power dissipation in memory devices is due to the leakage current through the gate dielectric material [5]. Thus, to reduce the power dissipation and for obtaining a better charge retention of DRAM a low leakage current is essential. Among the various approaches to optimize the properties in BST thin films, recently, a multilayer structure with a combination of BST and other dielectrics has been proven to be useful approach to improve the properties of BST film. Among the different approaches to reduce the leakage current in BST thin film, a multilayer with a combination of BST and ZrO_2 has been proven to be very useful approach. The conduction current is one of the most important issues for capacitor charge retention. In order to fully understand the conduction current,

the carrier transport mechanisms should be studied thoroughly.

Leakage current analysis in the dielectric thin film has been an important study for the use of these materials in microelectronic devices. The conduction mechanisms in thin films can be classified into two groups such as interfaced-controlled including Schottky emission, Fowler-Nordheim (FN) tunneling and bulk-controlled including Poole-Frenkel emission, space-charge-limited conduction (SCLC), and Ohmic conduction process [6]. Lots of work has been done to reduce the leakage current in BST thin films such as the heterostructured BST/MgO thin films [7]. However, the ohmic conduction mechanism in pure BST films and BST/ZrO_2/BST multilayred films and the study of activation energies have not been reported in detail yet.

In this work, the leakage current in BST films and BST/ZrO_2/BST multilayer thin films has been measured in the temperature range of 400 to 450K. The conduction mechanisms contributing to the leakage current in different field regions and the activation energy for electrons in the Ohmic conduction process in these films have been studied.

1.1 Simple structure of DRAM device

In 1968, R. H. Dennard of IBM patented the concept of the DRAM. His concept included one transistor and one storage capacitor, more commonly referred to as the one transistor (1-T) DRAM cell as shown in Figure 1.1. In DRAM cell, the capacitor will store the charge or data whereas the transistor will act as a control switch.

1.2 Charge storage capacity of the capacitor in a DRAM cell

The charge stored in a capacitor (Q) is given by Equation (1.1),

$$Q = C \times V \tag{1.1}$$

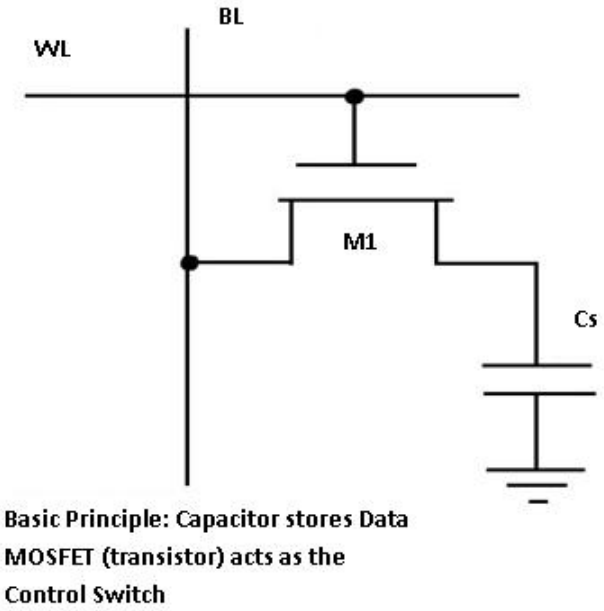

Figure 1.1: Simple structure of DRAM device.

where C is the capacitance of the capacitor at fixed voltage V. The expression for capacitance for a parallel plate capacitor is given by Equation (1.2),

$$C = \varepsilon_0 \varepsilon_r \frac{A}{d} \tag{1.2}$$

where C is the capacitance of the capacitor, ε_r is the dielectric constant, ε_0 is the permittivity of the free space, A is the cross-sectional area of the plate, d is the thickness of the dielectric layer in the capacitor. To increase the charge storage capacity of a capacitor, one has to increase the capacitance of the capacitor. It is seen that by simply decreasing the dielectric thickness, a higher capacitance can be achieved. If we are using conventional dielectric such as SiO_2, decreasing dielectric thickness will give more leakage current which is not good for the reliability performance of DRAM. Thus, it is not practical to focus on SiO_2 as the dielectric material for storage capacitor. Another option is to increase the cross sectional area of the capacitor. Unfortunately, there is more difficulty in the fabrication of these structures. The final option for increasing the capacitance is to use a material with a higher dielectric constant. Barium strontium titanate (BST) is a material which has high dielectric constant.

1.3 Charge retention capacity of the capacitor

Charge retention capacity of a capacitor is defined as the time duration for which the capacitor can hold the charge. If the charge loss of the capacitor is lower which means the charge retention capacity is higher. This charge retention capacity depends on the leakage current of the capacitor. Therefore, in order to improve the charge retention capacity, one has to reduce the leakage current of the capacitor.

1.4 Different leakage current mechanisms in the dielectric

1.4.1 Ohmic conduction mechanism

In the low electric field region, the possible leakage mechanism is Ohmic conduction which is carried out by thermally excited electrons hopping from one state to the next within the band gap of the dielectric as shown in Figure 1.2. When a positive field is applied to the top electrode (Au) of the MIM capacitor, electron will flow from the bottom electrode (Pt) to a defect state in the dielectric and then it will hop to the next defect state. As a result, the electron will go through the whole dielectric layer and will reach the top electrode.

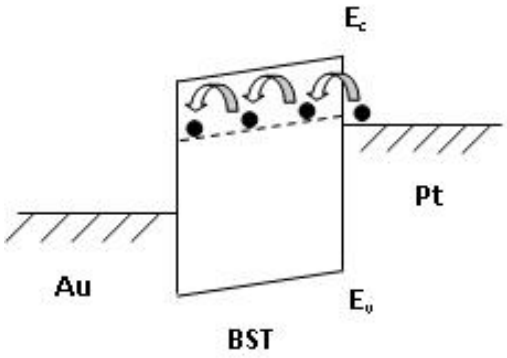

Figure 1.2: Schematic diagram showing the Ohmic conduction mechanism within a dielectric material.

The Ohmic J current density is given by Equation (1.3),

$$J \sim Eexp\left(\frac{-E_a}{kT}\right) \tag{1.3}$$

where E is the electric field, T is the device temperature, and E_a is the thermal activation energy of conduction electrons.

1.4.2 Space charge limited current (SCLC) mechanism

In the medium electric field region, space charge limited current (SCLC) mechanism occurs. When a positive voltage is applied to the top electrode (Au) of the MIM capacitor, the injected electrons from the bottom electrode (Pt) enter the conduction band of the dielectric layer, which form space charges. In a perfect, trap free insulator, all the injected electrons remain free and contribute to the space charge current. However, for dielectric films, traps are generally formed as a result of a large amount of structural disorders. The presence of empty traps in the dielectric film could significantly reduce the current by capturing a great portion of the injected electrons. This is called space charge limited current. As the applied voltage is increased, the traps will become filled gradually until a trap filled limited voltage (V_{TFL}) is reached where all the traps will eventually become filled. The SCLC mechanism is shown in the Figure 1.3.

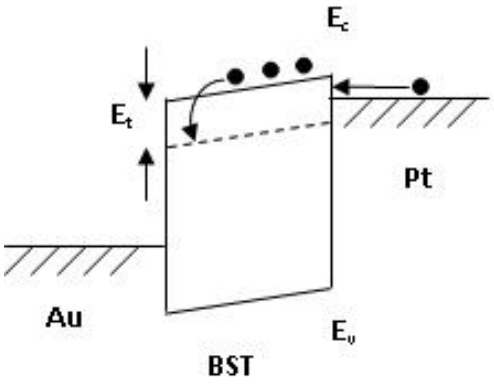

Figure 1.3: Schematic diagram showing space charge limited current (SCLC) mechanism within a dielectric material.

Assuming a single trap level below the conduction band of the dielectric, the relationship between the current density (J) and electric field (E) is given by Equation (1.4),

$$J = \frac{9}{8}\mu\varepsilon_0\varepsilon_r\theta\frac{E^2}{d} \tag{1.4}$$

where ε_r is the relative dielectric constant, ε_0 is the permittivity of the free space, μ is the electron mobility, E is the applied electric field, d is the film thickness, and θ is the ratio of free to trapped charges.

1.4.3 Poole-Frenkel mechanism

In the high electric field region Poole-Frenkel mechanism occurs. When high positive voltage is applied to the top electrode (Au) of the MIM capacitor, the injected electrons from the bottom electrode (Pt) will be trapped in the trap level present below the conduction band of the dielectric and then detrapped into the conduction band as shown in Figure 1.4. It is well known that the Poole-Frenkel

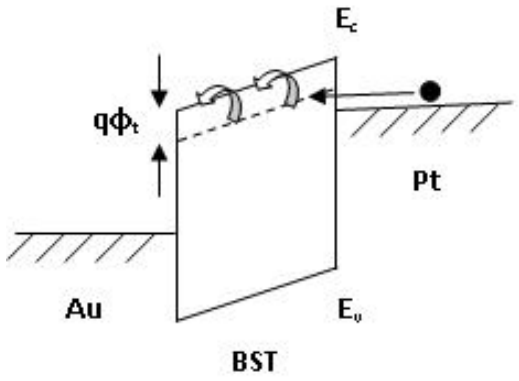

Figure 1.4: Schematic diagram showing the Poole-Frenkel (PF) mechanism within a dielectric material.

mechanism is due to the field enhanced thermal excitation of trapped electrons into the conduction band. Defects below the conduction band within the dielectric bandgap can participate in the conduction process through electron trapping and detrapping when both field and temperature are varied. The leakage current

density (J) due to Poole-Frenkel mechanism is described by Equation (1.5),

$$J_{PF} = qN_c\mu E exp\left(\frac{\beta_{PF}E^{\frac{1}{2}} - q\phi_t}{kT}\right) \tag{1.5}$$

where $\beta_{PF} = \left(\frac{q^3}{\pi\varepsilon\varepsilon_0}\right)^{\frac{1}{2}}$ (ε is the dynamic dielectric constant and ε_0 is the permittivity of the free space), N_c is the density of states in the conduction band, μ is the electron mobility, $q\phi_t$ is the trap level energy, E is the electric field, k is the Boltzmann constant, and T is the device temperature.

1.5 (Ba,Sr)TiO_3 dielectric material

To store more data in DRAM the capacitance of a capacitor have to increase. The suitable option for increasing the capacitance of a capacitor is to use a material with higher dielectric constant. The search for materials having higher dielectric constants have led to ferroelectric materials, since the permittivity of these materials can be a few hundred times higher than that of SiO_2. Ferroelectric materials were discovered and have been studied since 1921, but have not been seriously considered for semiconductor memory application till now. BaTiO_3 is a ferroelectric material and has been well studied in bulk ceramic form. The utilization of the BaTiO_3-SrTiO_3 solid solution allows the Curie temperature (ferroelectric-paraelectric transition temperature, Tc) of BaTiO_3 to be shifted from 120^{o}C to around room temperature for $Ba_{1-x}Sr_xTiO_3$ material. Generally, the ferroelectric materials show high dielectric constant at the transition temperature. By the addition of Sr into pure BaTiO_3, the transition temperature can be brought down to room temperature. Therefore, we will get a high dielectric constant at room temperature for $Ba_{1-x}Sr_xTiO_3$ material. In this material, x is used as the composition of Sr. In this research work, we have added 20 mol% of Sr (i.e, x = 0.2) into pure BaTiO_3 so that we have used $Ba_{0.8}Sr_{0.2}TiO_3$ (BST) as the dielectric material.

1.6 Related Work

Dielectric Characteristics of Barium Strontium Titanate Based Metal Insulator Metal Capacitor for Dynamic Random Access Memory Cell [8].

- The Metal-Insulator-Metal (MIM) capacitor structure is designed and fabricated with barium strontium titanate (BST) oxide material as the capacitor dielectric material and silver as both top and bottom electrodes for dynamic random access memory (DRAM) cell.
- This designed capacitor consists of about 2 mm BST pellet and about 1 mm silver top and bottom electrodes.
- The composition of the BST is chosen as $Ba_{0.5}Sr_{0.5}TiO_3$ due to its better dielectric characteristics as shown in Figure 1.5.
- The dielectric characteristics of both the fabricated MIM and the simulated MIM are compared and it is found that the experimental values and simulated values are found to be comparable. The simulated dielectric constant, dielectric loss, charge storage density, leakage current density are found to be 1250, 0.025, 5 $\mu C/cm^2$ and 5 pA/cm^2, respectively against the corresponding experimental values of 1164, 0.063, 3.5 $\mu C/cm^2$ and 49.4pA/cm^2.

Preparation and characterization of (Ba,Zr)TiO_3/(Ba,Sr)TiO_3 heterostructure grown on $(LaAl\ O_3)_{0.3}$ $(S\ r_2\ \mathrm{AlTa}O_6)_{\ 0.35}$ single crystal substrates by pulsed laser deposition [9].

- (Ba,Sr)TiO_3, Ba(Zr,Ti)O_3 single layer films and (Ba,Sr)TiO_3/ (Ba,Zr)TiO_3 multilayered films are deposited and their dielectric properties are studied.
- It is observed that dielectric constant for multilayered films is lower compared to that of single layer films due to the series combination of two capacitors as shown in Figure 1.6.

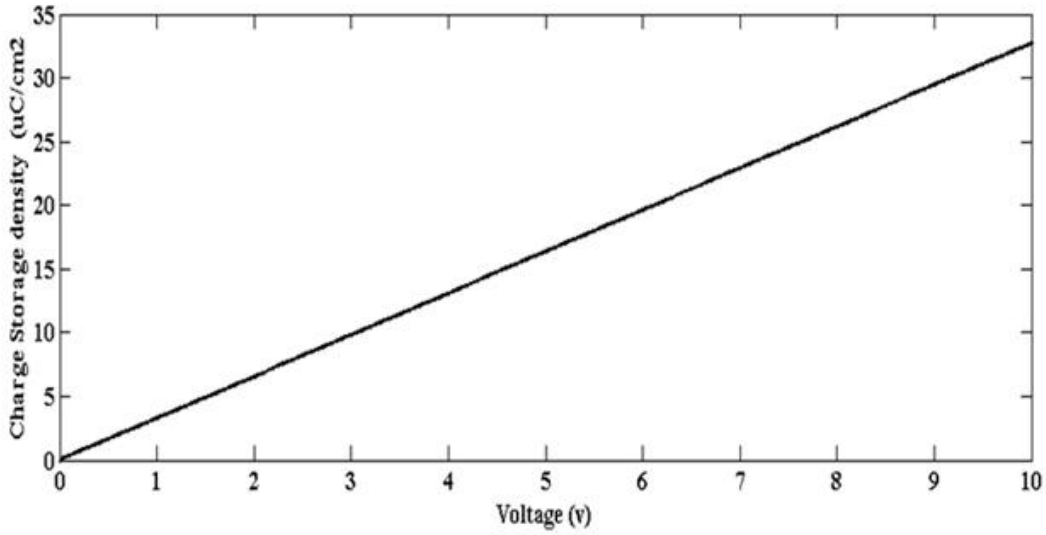

Figure 1.5: Charge storage density vs. voltage for BST capacitor.

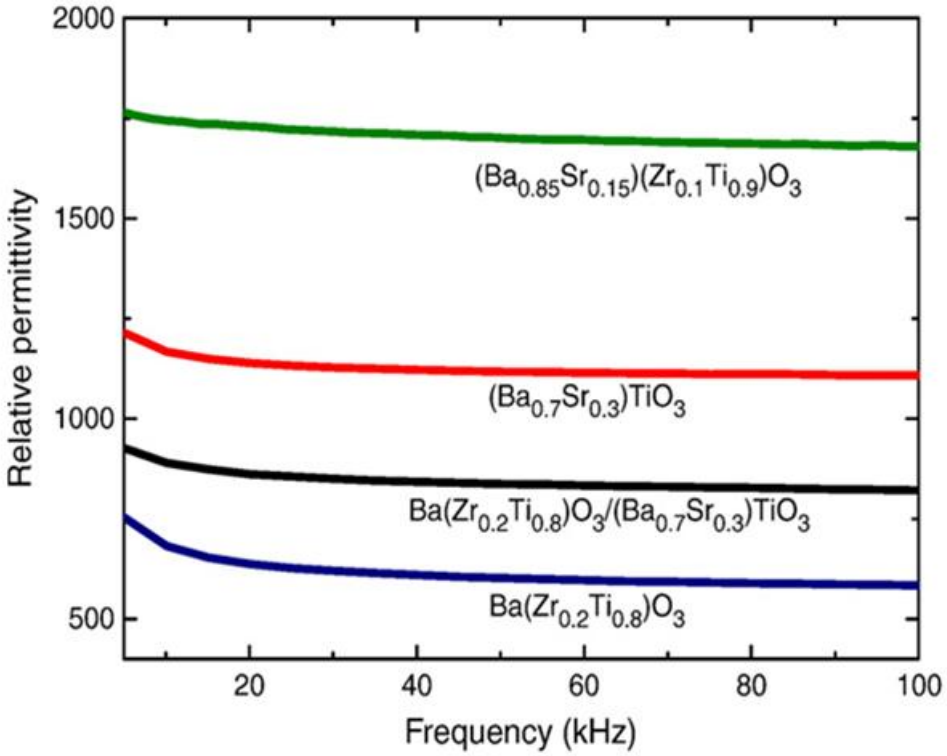

Figure 1.6: Relative permittivity vs. frequency for BST, BZT, BZT/BST and BSZT thin films.

- Also multilayered films show good tunability of 44% whereas single layer films show 39%.
- Therefore, multilayered dielectric films are showing better dielectric properties compared to those of single layer films.

Dielectric properties of sol-gel derived MgO:$Ba_{0.5}Sr_{0.5}TiO_3$ thin film composites [10].

- (Ba,Sr)TiO_3/MgO multilayered dielectric thin films are deposited by sol-gel process and their dielectric properties are studied for microwave device applications.
- Dielectric constant and dielectric loss is a function of temperature for BST films and BST/MgO multilayered films as shown in Figure 1.7.
- It is observed that BST/MgO multilayered dielectric films show improved dielectric properties such as low dielectric loss (tanδ) = 0.0049 and K $factor = 51.42$ compared to those of single layer BST dielectric films.

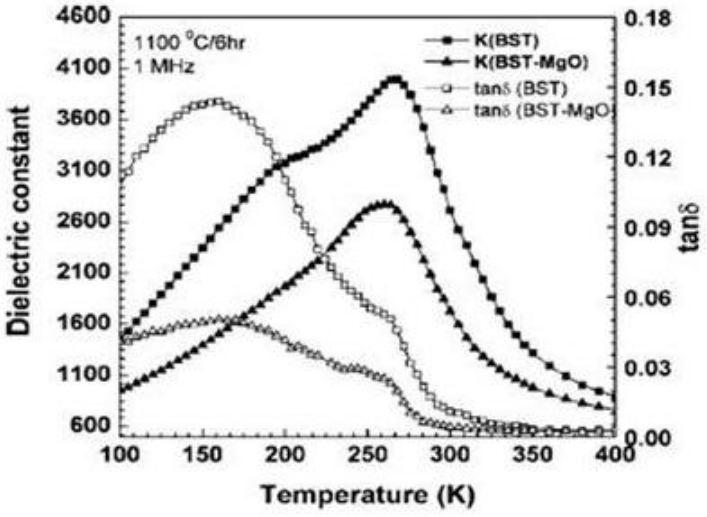

Figure 1.7: Dielectric constant and dielectric loss as a function of temperature for BST films and BST/MgO multilayered films.

Substantial reduction of the dielectric losses of $Ba_{0.6}Sr_{0.4}TiO_3$ thin films using a SiO_2 barrier layer [11].

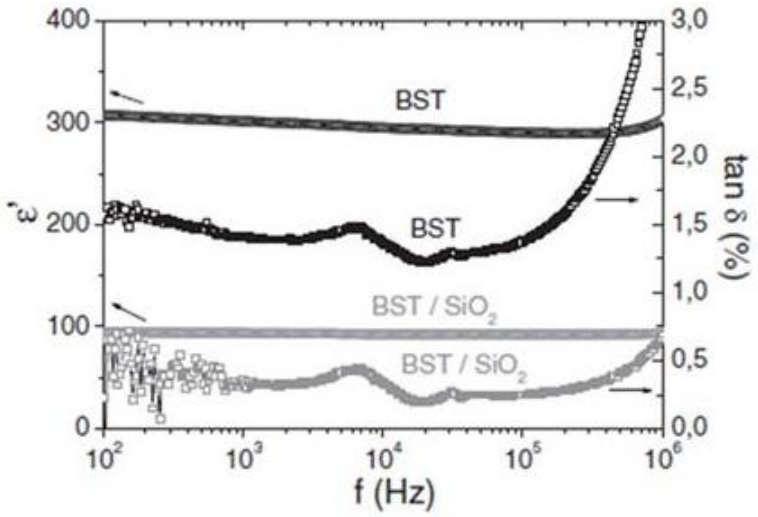

Figure 1.8: Frequency dependence of relative permittivity and dielectric loss for BST films and BST/SiO_2 bilayered film.

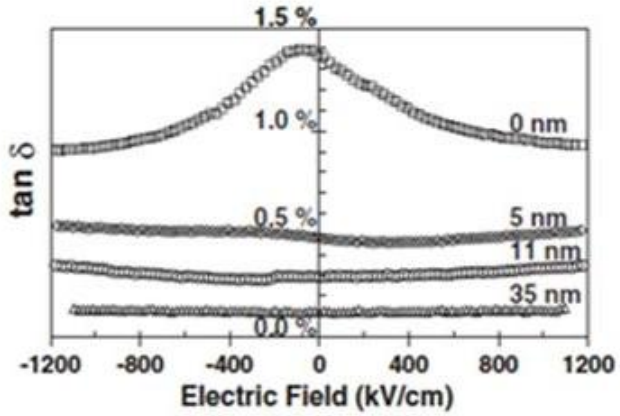

Figure 1.9: Dielectric loss vs. electric field for BST films and BST/SiO_2 bilayered films with different SiO_2 thicknesses.

- The improvement in dielectric loss parameter in dielectric thin films for applications in dynamic memory and microwave devices are studied.

- The single layered $(Ba, Sr)TiO_3$ films and multilayered $(Ba, Sr)TiO_3/SiO_2$ are deposited by sputtering technique.
- The multilayered films show low dielectric loss compared to that of single layer films as shown in Figure 1.8.
- BST/SiO_2 multilayered films show better dielectric performance as shown in Figure 1.9.

Improvement in electrical characteristics of graded manganese doped barium strontium titanate thin films [12].

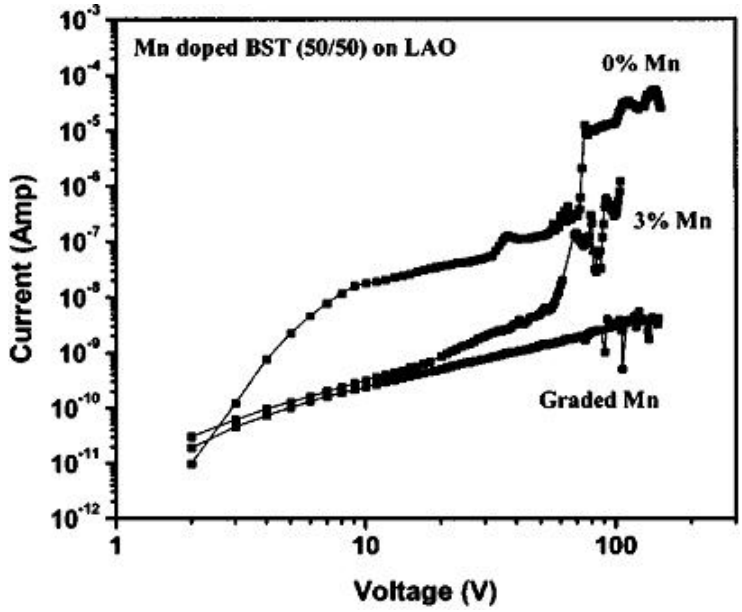

Figure 1.10: Comparison of current vs. voltage of Mn doping to pure BST films.

- The effect of Mn on the leakage current of (Ba,Sr)TiO_3 thin films. They observed that the leakage current decreases with Mn doping in comparison to pure BST films.
- Comparison of current vs. voltage of Mn doping to pure BST films is shown in Figure 1.10.

Chapter 2

Study of different conduction mechanisms to increase the performance of DRAM

- Study of leakage current in BST films and proposition of BST/ZrO_2/BST multilayer thin films in the temperature range of 400 to 450K.
- The conduction mechanism contribution to the leakage current in low field region and the calculation of activation energy for electrons.

2.1 I-V measurements of a capacitor

Keithley 6517A electrometer is used to take the I-V measurements of the MIM capacitors.

The HI terminal from the rear panel of the electrometer is connected to the top electrode (Au) of the capacitor whereas the LO terminal is connected to the bottom electrode (Pt) of the capacitor for taking I-V measurements. The IEEE-488 terminal from the real panel of the electrometer is connected to the

computer to take the I-V measurements automatically using LABVIEW programs as shown in Figure 2.1.

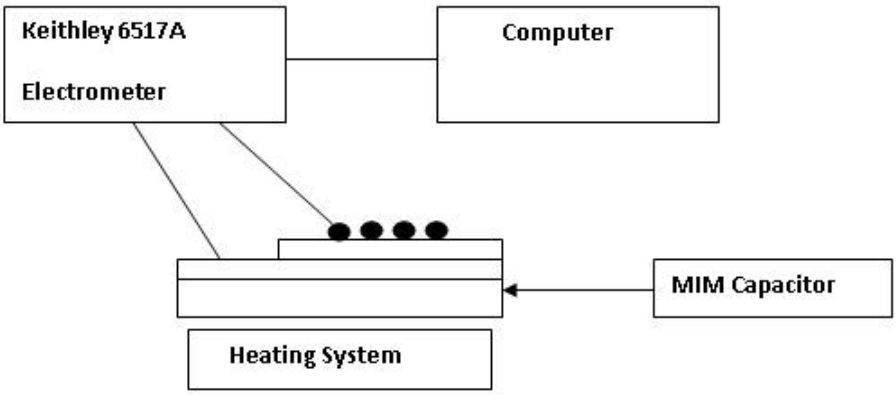

Figure 2.1: Schematic diagram of the I-V measurement systems.

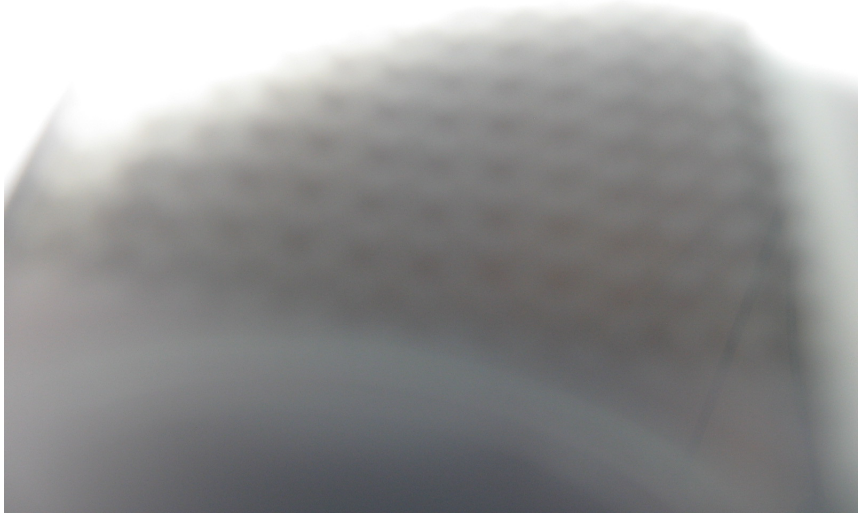

Figure 2.2: Diagram of the sample for I-V measurement.

2.2 I-V measurements of a standard capacitors

DC Power supply is given to a standard capacitor. The voltage change is made by the knob present in the supplier and one ammeter is also connected to the

capacitor to read the current value with respect to voltage change.

2.3 Activation energy calculation

The current density (J) due to Ohmic conduction is given by,

$$J \sim Eexp\left(-\frac{E_a}{kT}\right) \tag{2.1}$$

Taking natural logarithm (ln) of both the sides of the above equation, we will get,

$$lnJ = lnE - \frac{E_a}{kT} \tag{2.2}$$

$$lnJ = lnE + \left(-\frac{E_a}{k}\right)\left(\frac{1}{T}\right) \tag{2.3}$$

$$lnJ = lnE + \left(-\frac{E_a}{k \times 1000}\right)\left(\frac{1000}{T}\right) \tag{2.4}$$

At a fixed electric field, by plotting lnJ on the y-axis and 1000/T on the x-axis, we will get a straight line and the slope of this line is given by,

$$slope = -\frac{E_a}{k \times 1000} \tag{2.5}$$

$$E_a = (-slope) \times k \times 1000 \tag{2.6}$$

$$E_a = (-slope) \times 8.617 \times 10^{-5}\frac{eV}{K} \times 1000 \tag{2.7}$$

$$E_a = (-slope) \times 8.617 \times 10^{-2}eV \tag{2.8}$$

$$E_a = (-slope) \times 0.08617eV \tag{2.9}$$

If the slope of the linear fitting is known, the activation energy can be calculated using the Equation 2.9.

2.4 Simulated leakage current of Au/BST/Pt capacitor of DRAM

(Ba,Sr)TiO_3 (BST) is a high dielectric constant material which is used in metal-insulator-metal (MIM) capacitor for dynamic random access memory (DRAM) applications. The dielectric material should have high dielectric constant as well as low leakage current for its application in DRAM devices. The high dielectric constant will give higher capacitance density and hence more charge storage in the capacitor. Leakage current is an important parameter which determines the charge retention capacity of the capacitor. Also this leakage current evaluates the power loss in memory circuits. In order to better understand the application of a dielectric material in MIM capacitor for DRAM applications, it is very important to estimate the simulated leakage current in a capacitor. In this work, we have studied the electric field dependent leakage current density (J versus E) in Au/BST/Pt MIM capacitor. Poole-Frenkel (PF) conduction mechanism is a well known process for the leakage current in high dielectric constant materials. The leakage current due to PF process is given by Equation (2.2),

$$J_{PF} = qN_c\mu E exp\left[\frac{-q\left(\phi_t - \sqrt{\frac{qE}{\pi\varepsilon_r\varepsilon_0}}\right)}{kT}\right] \tag{2.10}$$

where μ is the electron mobility, E is the electric field, q is the charge, N_c is the effective density of states, ϕ_t is the trap level energy, ε_r is the dynamic dielectric constant, and T is the temperature. For theoretical calculation of leakage current, we have taken the thickness of the BST dielectric thin film as 380 nm and used different voltage range. The electric field is calculated as E = V/ thickness. We have done the simulation in the temperature range of 400 to 450K. We have used the following values for different parameters which are collected from literatures and used in Equation (2.10) in order to estimate the simulated leakage current in BST dielectric.

μ = 1.0 x 10^{-14} m^2/V s

N_c = 1.0 x 10^{24} m^{-3}

q = 1.602 x 10^{-19} C

$\varepsilon_r = n^2 = 4$

ε_0 = 8.85 x 10^{-12} F/m

ϕ_t = 0.54 eV

T = 400 K to 450 K

k = 1.38 x 10^{-23} J/K

The trap level energy (ϕ_t) has been calculated from our experimental data shown in Figure 2.3.

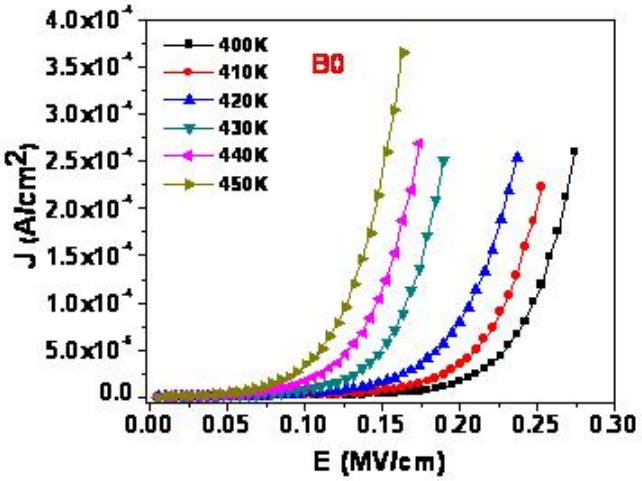

Figure 2.3: Experimental J vs. E at different temperature for B0 sample.

In order to calculate the trap level energy, we have plotted ln(J/E) vs $E^{0.5}$ as shown in Figure 2.4 It is observed that the high field region data are in a straight line. We made a linear fit in the high field region. We obtained the slope and y-intercept from the linear fit in Figure 2.4. Thereafter, we plotted the y-intercept versus 1000/T in Figure 2.5. Again we made a linear fit as shown in Figure 2.5. We calculated the trap level energy from the slope of the linear fit in Figure 2.5. The estimated trap level energy (ϕ_t) comes out to be 0.54 eV. We used this trap level energy for the estimation of simulated leakage current density in the MIM capacitor using BST dielectric.

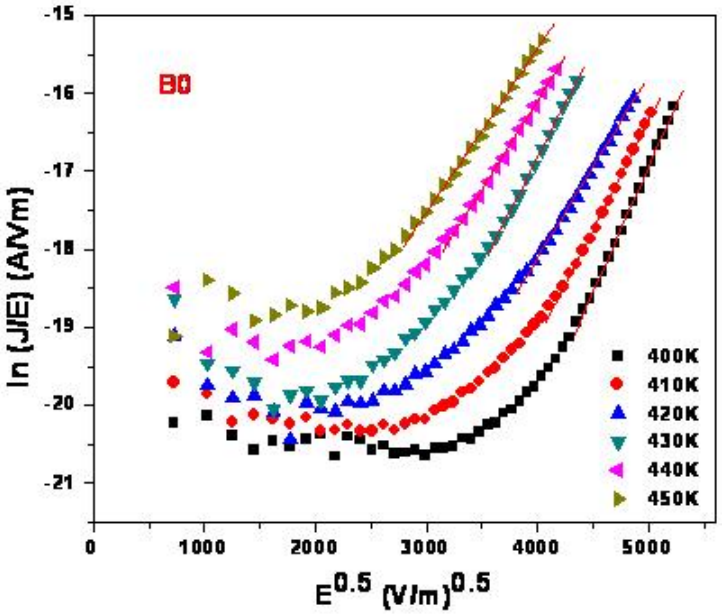

Figure 2.4: ln(J/E) vs. $E^{0.5}$ at different temperature for B0 sample.

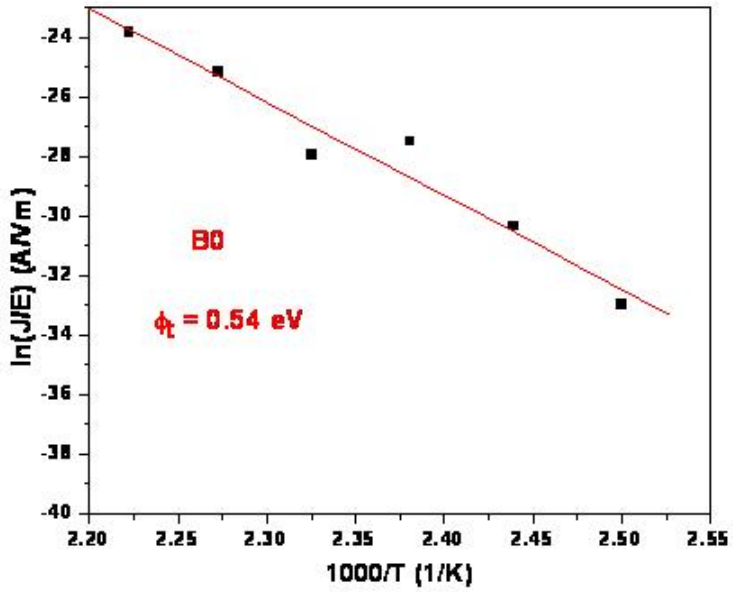

Figure 2.5: ln(J/E) vs. 1000/T for B0 sample.

The simulated leakage current density (J) versus electric field (E) for Au/BST/Pt MIM capacitor at different temperatures is shown in Figure 2.6.

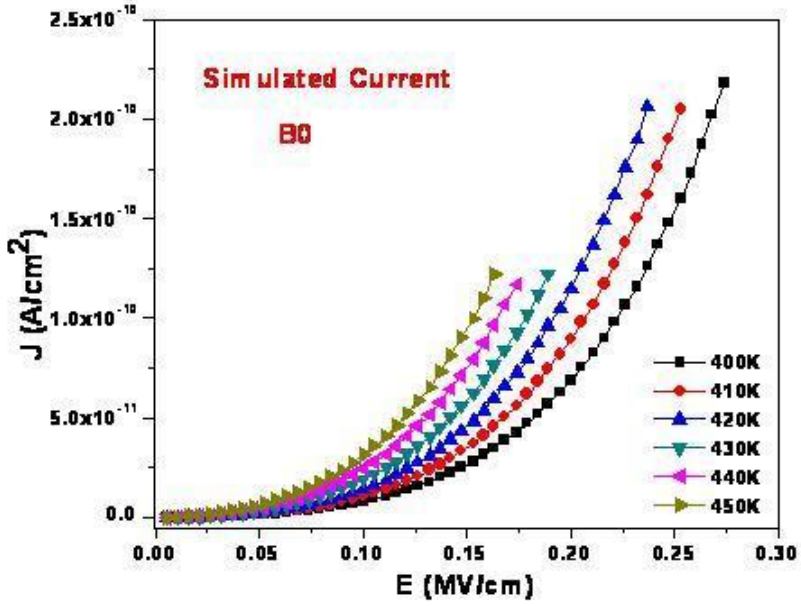

Figure 2.6: Plot of simulated J vs. E for Au/BST/Pt MIM capacitor at different temperatures.

2.5 Experimental value analysis using Origin software and collected using Labview

The Labview software from national instruments (NI) is installed in the computer and a Labview program is used to take the I-V measurements for the capacitor devices. On the front panel of the Labview program, an intial voltage of 0.2 V and a final voltage of 10.0 V are given for the measurement at a particular temperature. Different final voltages are used for various temperatures. A step voltage of 0.2 V is given so that the current is measured at different voltages such as 0.2 V, 0.4 V, 0.6 V, 0.8 V, 1.0 V, ..10.0 V at fixed temperature. Similarly, the I-V measurents are taken at other temperatures. For the measurement at each step voltage, a time delay of 100 ms is given. After one complete measurement, the data is transferred automatically from the measuring instrument to the controlled computer. The stored I-V data in the computer has been further analyzed for this thesis work.

Figure 2.7 shows the measured capacitance and dielectric loss at different frequencies for an MIM capacitor using Labview program. Figure 2.8 shows the experimental leakage current (I) at different voltages (V) for an MIM capacitor using Labview program. Figure 2.9 shows the block diagram of the Labview program for the measurement of leakage current (I) at different voltages (V) for an MIM capacitor. Figure 2.10 shows the commands for thae measurement of leakage current (I) at different voltages (V) for an MIM capacitor using Labview program.

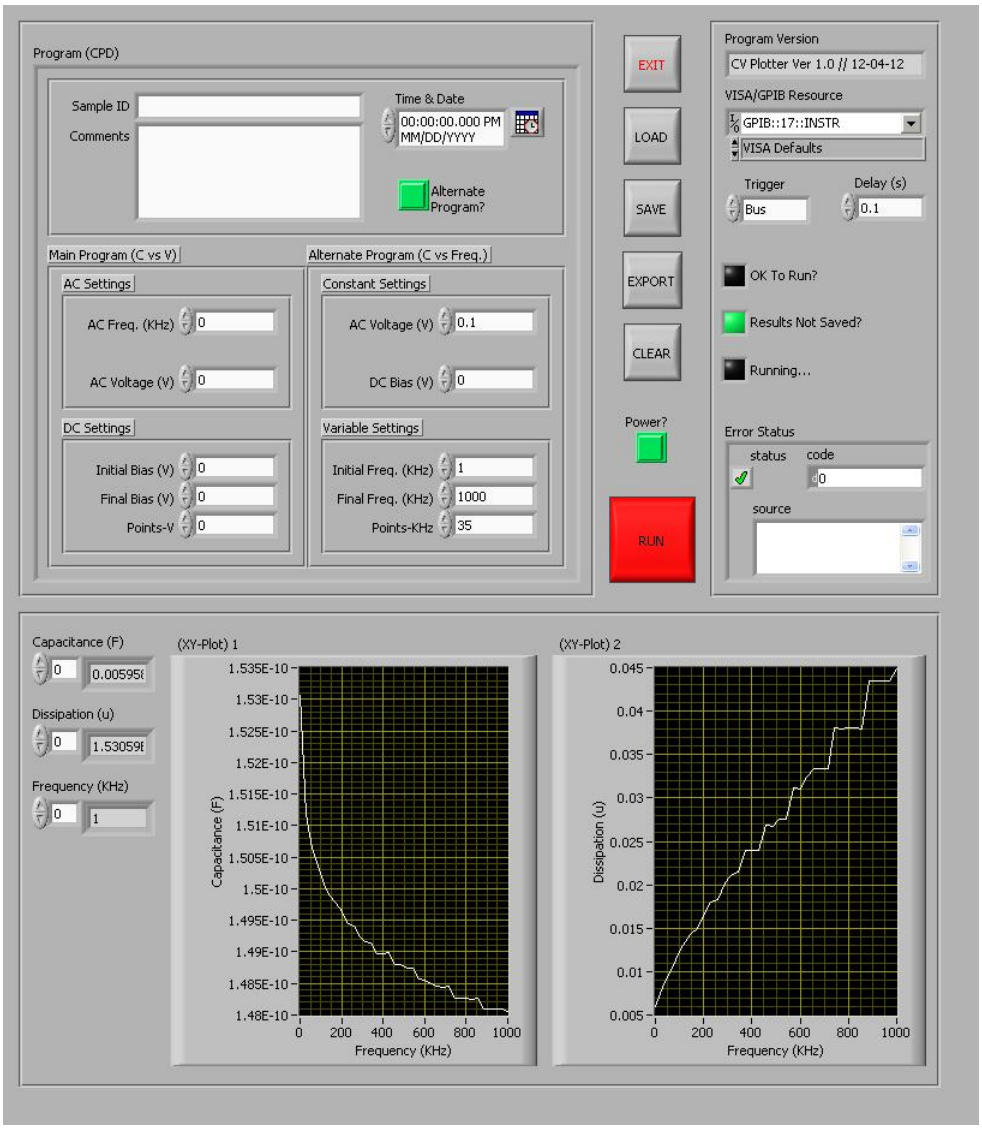

Figure 2.7: Test-1

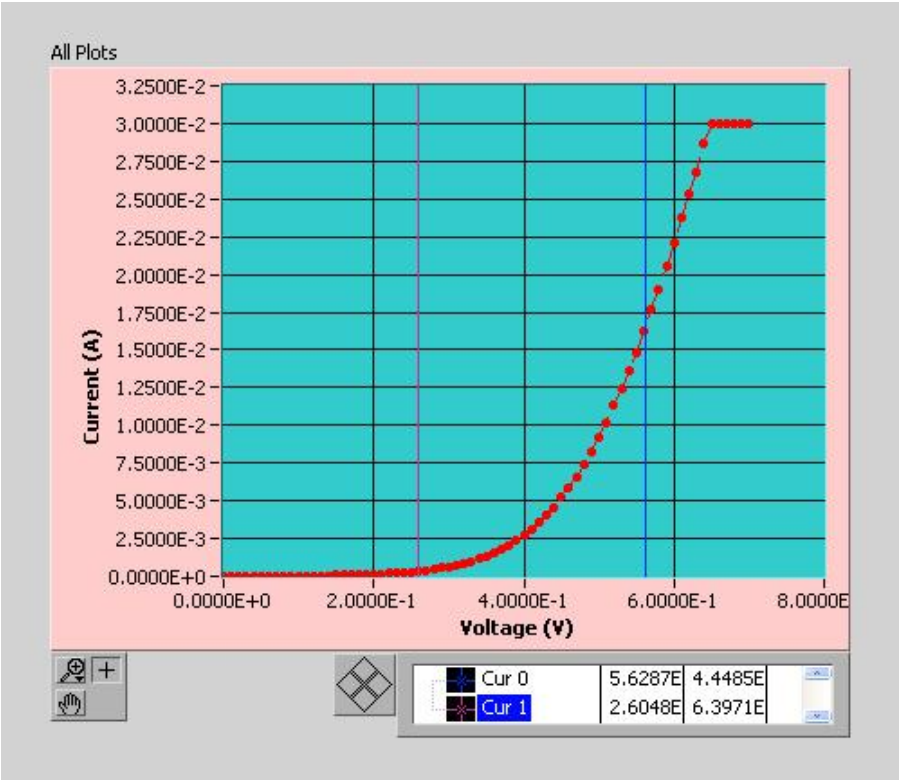

Figure 2.8: Export of Test-1

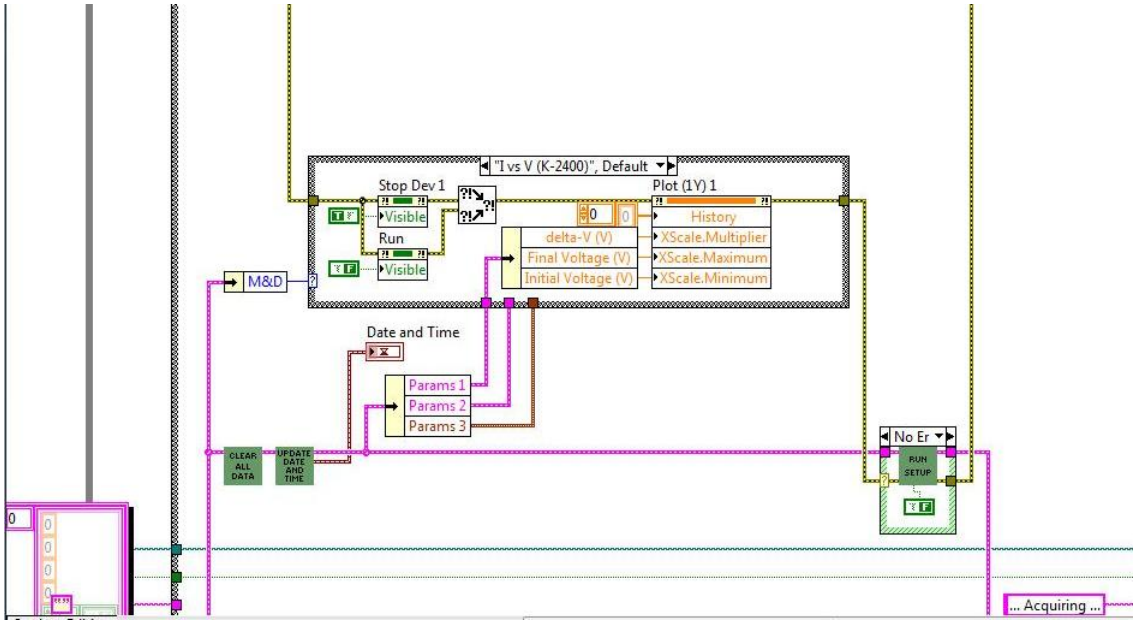

Figure 2.9: Block diagram for I-V measurements.

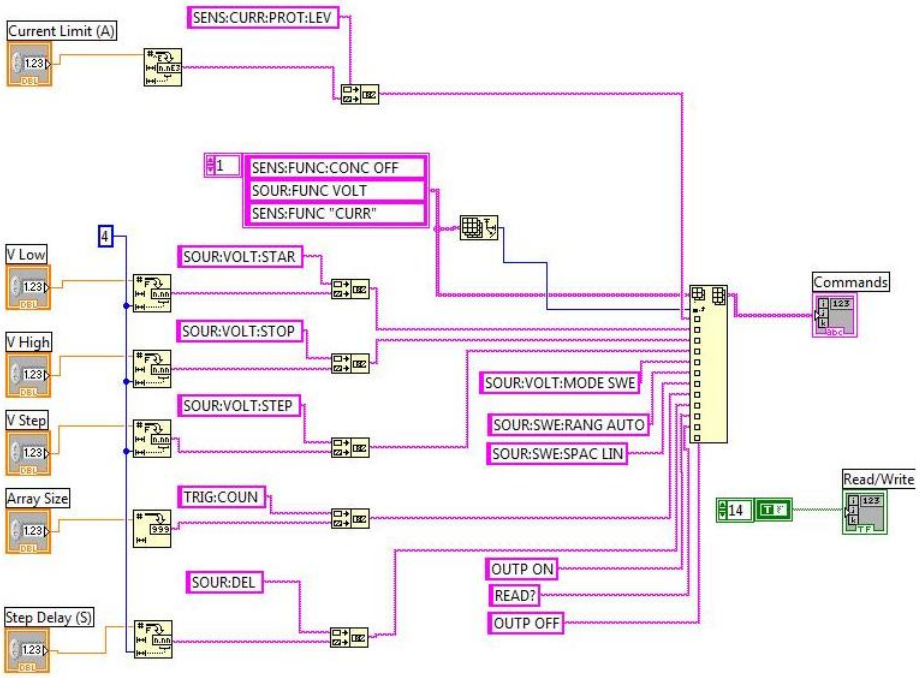

Figure 2.10: Block diagram showing different commands for I-V measurements.

2.6 Different sample structure

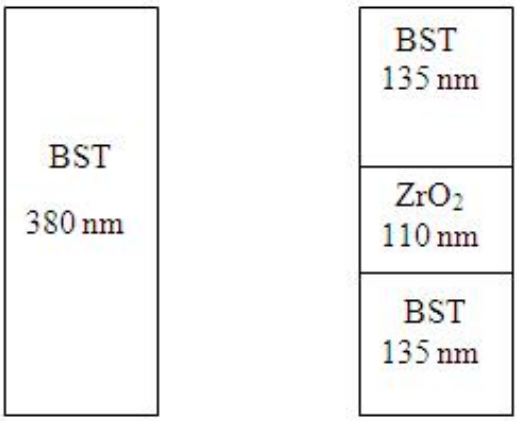

Figure 2.11: Schematic diagrams of pure BST film and BST/ZrO_2/BST multilayered films structure.

Chapter 3

Results and Discussion

3.1 J vs. E plot for BST and BST/ZrO_2/BST film at different temperatures

Figure 3.1 shows the leakage current density (J) versus electric field (E) plots in the temperature range of 400 - 450K for BST films and $BST/ZrO_2/BST$ multilayered films. It is observed that J increases with the increase of temperature. The strong temperature dependence of the leakage current density (Figure 3.1 (a) and (b)) suggests that the electron transport is activated such as one would expect either an Ohmic conduction process or space charge limited current (SCLC) mechanism is contributing to the leakage current in the low field region in these multilayered films.

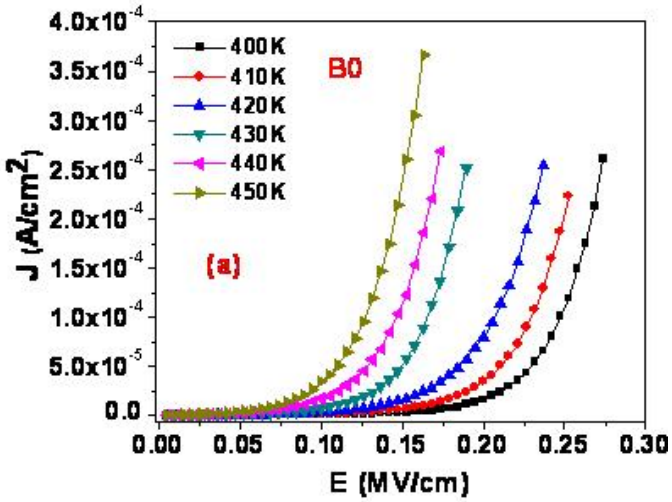

(a)

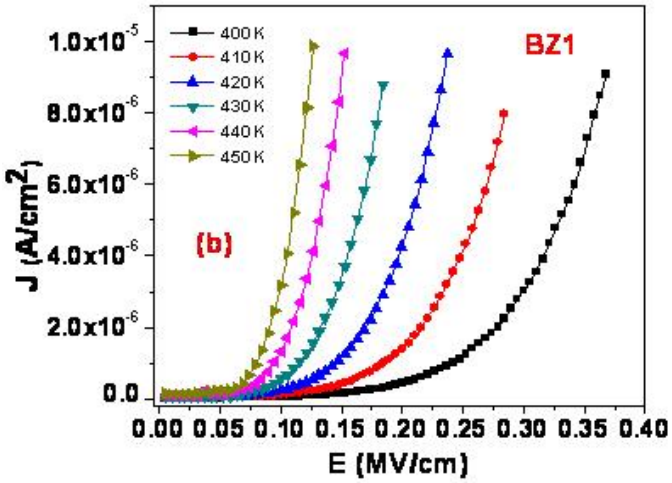

(b)

Figure 3.1: J vs. E plot for (a) BST (B0) film and (b) BST/ZrO_2/BST (BZ1) multilayered film at different temperatures.

3.2 lnJ vs. lnE plot for BST and BST/ZrO_2/BST film at different temperatures.

To explain the different conduction mechanisms contributing to the leakage current in this dielectric films, the temperature dependent J-E data as shown in Figure 3.1 is plotted as lnJ versus lnE in Figure 3.2 for BST and BST/ZrO_2 multilayered films, respectively. From Figure 3.2, it is observed that the slope is close to 1 in the low electric field region. Therefore, it is possible that some mechanism is contributing to the leakage current in the low field region. It is also known that Ohmic conduction process is observed when the volume generated intrinsic free carrier density, n_0, is higher than the injected free carrier density, n_i. It is observed that the slope of the ln J vs. ln E curve is slightly smaller than 1 for both BST films and BST/ZrO_2 multilayer films, in the low field region, which probably resulted from the ferroelectric polarization of BST thin film [13].

As the leakage current density is temperature dependent (Figure 3.1) also in the low field region, the direct tunneling mechanism is ruled out. At this low field regime, the possible leakage mechanism is Ohmic conduction which is carried by thermally excited electrons hopping from one state to the next. This Ohmic current density is given by Equation (3.1) [6]

$$J \sim Eexp\left(\frac{-E_a}{kT}\right) \tag{3.1}$$

where E is the electric field, T is the device temperature, and E_a is the thermal activation energy of conduction electrons. To further confirm the dominance of Ohmic conduction mechanism, the I-V data is plotted as ln J versus ln E according to Equation (3.1) and are shown in Figure 3.2. It can be seen that the I-V data in the low field regime perfectly fits to a straight line with a slope ~ 1. Hence, Ohmic conduction is the dominant mechanism in the low electric field region. Therefore, one can conclude that the conduction process through BST films and BST/ZrO_2 multilayered films is Ohmic in the low field region.

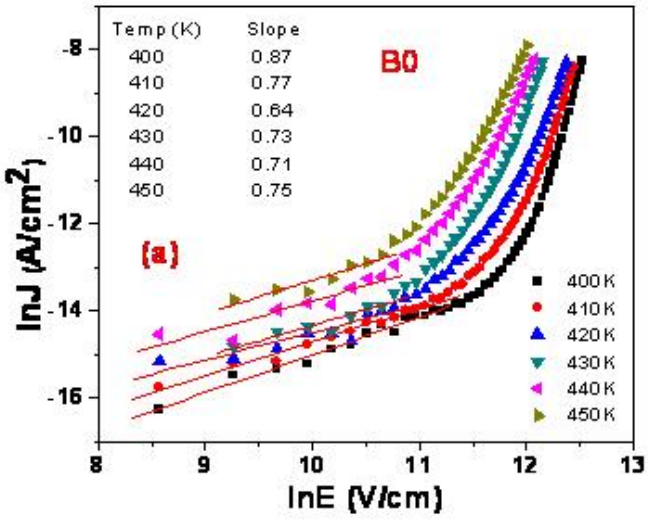

(a)

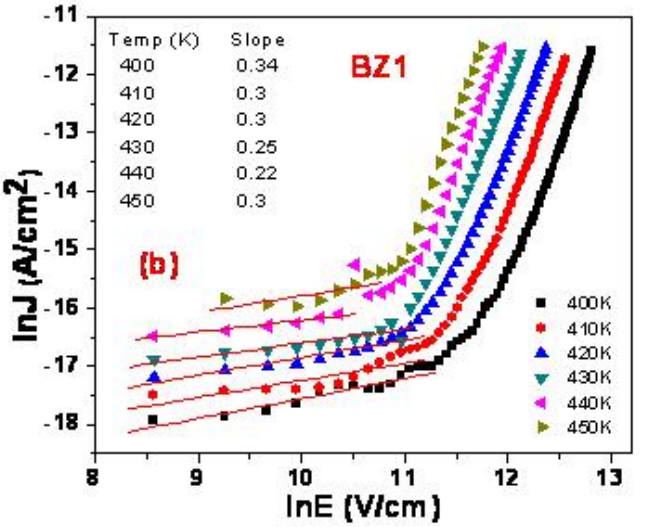

(b)

Figure 3.2: ln J vs. ln E plot for (a) BST (B0) film and (b) BST/ZrO_2/BST (BZ1) multilayered film at different temperatures.

3.3 lnJ vs. 1000/T plot for BST and BST/ZrO_2/BST film

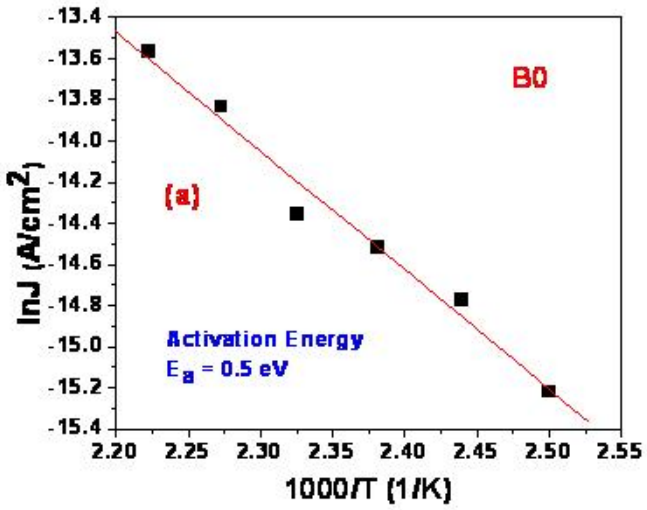

(a)

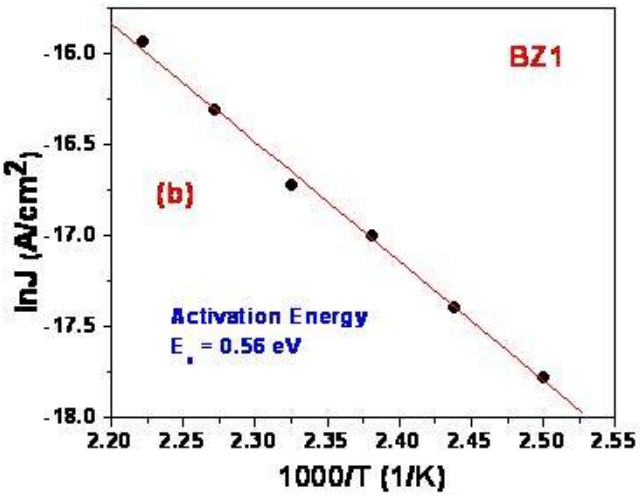

(b)

Figure 3.3: ln J vs.1000/T plot for (a) BST (B0) film and (b) BST/ZrO_2/BST (BZ1) multilayered film.

In the low field region where Ohmic conduction is dominant, the plot of ln J versus $1000/T$ gives a straight line at a fixed electric field as per Equation (3.1) and the slope determines the thermal activation energy (E_a) for the Ohmic conduction

mechanism. The activation energy was determined at a fixed electric field (0.21 x 10^5 V/cm) for both pure BST film and BST/ZrO_2 multilayered films. Figures 3.3 (a) and (b) show the plot for ln J versus $1000/T$ and the activation energies come out to be 0.5 and 0.56 eV for BST and BST/ZrO_2/BST films, respectively.These values are close to the reported activation energies by Liu et al. [14] and are very close to the energy required for the diffusion of doubly ionized oxygen vacancies ($V_o^{\cdot\cdot}$) which are the active electron traps for the conduction process in these films.

3.4 lnJ vs. lnE plots showing linear fitting in the medium field region for SCLC mechanism

In Figure 3.2, it is observed that the I-V data points in the medium field region are deviating from the linear fit of the low field region data. It looks like some other conduction mechanism rather than Ohmic is contributing to the leakage current in this region. When a single discrete trap level exists in the band gap, current density J dominated by SCLC mechanism is given by Equation (3.2) [6],

$$J = \frac{9}{8}\mu\varepsilon_0\varepsilon_r\theta\frac{E^2}{d} \tag{3.2}$$

where ε_r is the relative dielectric constant, ε_0 is the permittivity of the free space, μ is the electron mobility, E is the applied electric field, d is the film thickness, and θ is the ratio of free to trapped charge. According to Equation (3.2), lnJ versus lnE plot will give a straight line with a slope of 2. In order to examine the dominance of SCLC mechanism in the medium field region, we have plotted the $I-V$ data as lnJ vs. lnE as shown in Figure 3.4. It is observed that there is a linear fit in the medium field region and the slopes come out to be nearly 2 for all the temperatures. Therefore, SCLC mechanism is contributing to the leakage current in this region. Hence, we conclude that Ohmic and SCLC mechanism are dominant in the low and field regions, respectively for both BST and BST/ZrO_2/BST films. The voltage at the trap filled limit (V_{TFL}) is the voltage between quadratic (slope =2) and higher than quadratic SCLC (slope>2) regions when all the trap levels

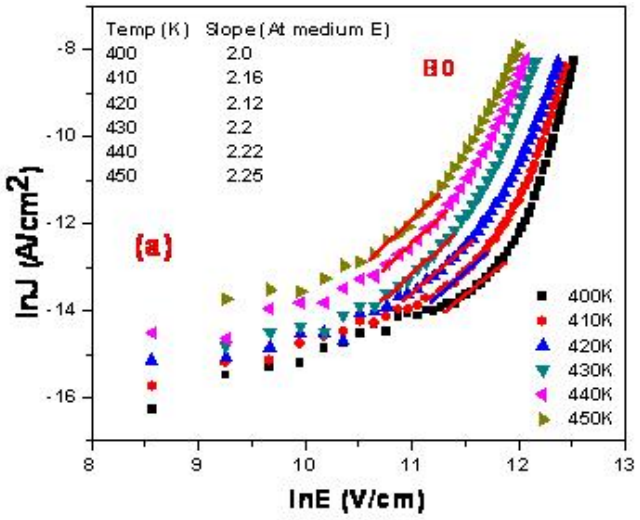

(a)

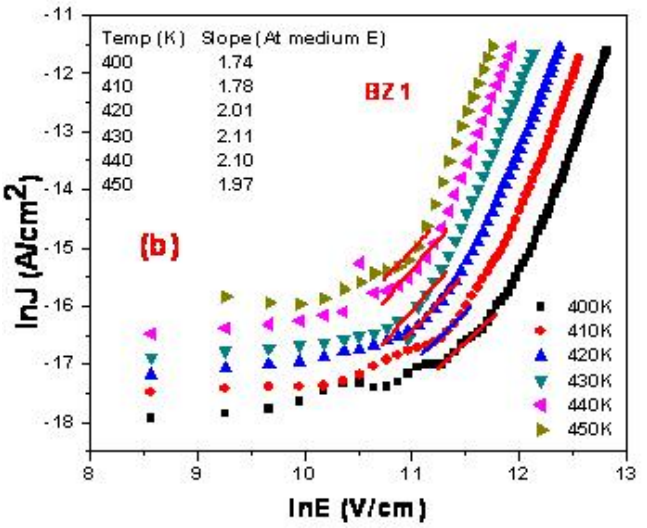

(b)

Figure 3.4: lnJ vs. lnE plots showing linear fitting in the medium field region for SCLC mechanism (a) (BST)B0 films and (b) BZ1 multilayered films.

are fully occupied. V_{TFL} can be expressed as [15]

$$V_{TFL} = \frac{qN_t d^2}{2\varepsilon_0 \varepsilon_r} \tag{3.3}$$

where N_t is the trap density, d is the thickness, and ε_r is the relative permittivity of the film. The trap concentration N_t calculated from V_{TFL} comes out to be 2.2 x 10^{18} cm^{-3} for BST/ZrO_2 multilayered films and 5.1 x 10^{18} cm^{-3} for pure BST films at room temperature. Hence, there is a reduction in trap density due to insertion of ZrO_2 layer in BST films. Therefore, multilayered films are better than the single layer films with respect to leakage current. Hence, the higher activation energy observed for BST/ZrO_2 multilayered films is due to the lower trap density in comparison to pure BST films [16].

3.5 Comparison of leakage current density (J) versus field (E) for B0 and BZ1 films at temperatures 400 and 410 K

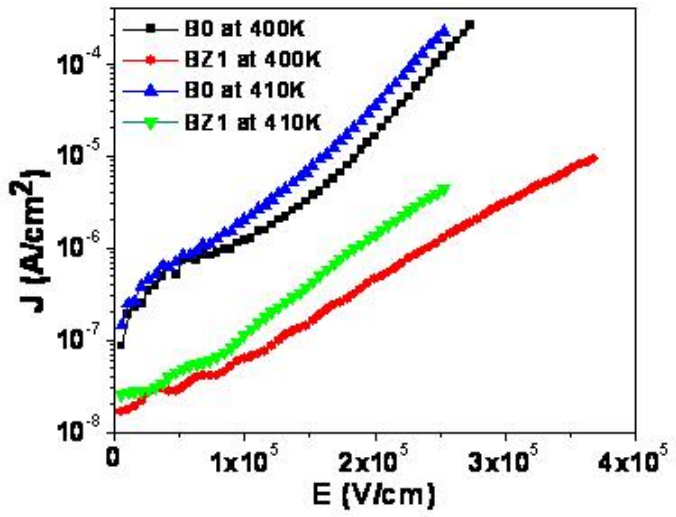

Figure 3.5: Comparison of leakage current density (J) versus field (E) for B0 and BZ1 films at temperatures 400 and 410 K.

The physical explanation for the possible origin of the conduction mechanism

in both BST films and $BST/ZrO_2/BST$ multilayered thin films is that, when low positive field is applied to the top electrode (Au), band bending occurs in the dielectrics [16]. The injected electrons from the bottom electrode (Pt) passes through the dielectric films and do not enter the trap level below the conduction band. Therefore, Ohmic conduction is the dominant mechanism in the low field region. When high positive field is applied, more band bending occurs and traps present below the conduction band participate in the conduction process. Hence, SCLC mechanism occurs at medium field region in these films [16].

Figure 3.5 shows the comparison of J vs. E plots for BST films and BST/ZrO_2 multilayered films at temperatures 400 and 410K. It is observed that the leakage current density is reduced by about one order of magnitude for BST/ZrO_2 films compared to that of pure BST films in the entire field range and is due to the increase in the activation energy for electrons and a reduction in trap density by the introduction of ZrO_2 layer in between BST layers in multilayered films.

Table 3.1: Comparison of leakage current.

Thin Films	Leakage Current (A) at 10 V	Reference	Summary
(Ba, Sr)TiO_3	$\sim 10^{-8}$	Jain et al. [12]	More leakage current
(Ba, Sr)TiO_3	$\sim 7.8^{-11}$	In our work	Less leakage current

From the above table, it is clear that our (Ba,Sr)TiO_3 films show low leakage current comparison to the results reported by Jain et al. [12].

Chapter 4

Conclusions and Future Work

In summary, the leakage current and conduction mechanisms are studied for both BST films and BST/ZrO_2/BST multilayered thin films fabricated on Pt/Ti/SiO_2/Si substrates by a sol-gel process. It is observed that in these films Ohmic conduction process is the dominant mechanism in the low field region whereas SCLC mechanism contributes to the leakage current in the medium field region. The activation energy for conduction electrons increases from 0.5 to 0.56 eV with the introduction of a ZrO_2 layer in between BST layers. The leakage current density is reduced by an order of magnitude for BST films with ZrO_2 layer compared to that of pure BST films in the whole field range. Therefore, BST/ZrO_2/BST multilayered dielectric films are very suitable for DRAM applications due their low leakage current density as well as low trap density in comparison to pure BST films. The higher measured leakage current observed compared to simulated leakage current for BST thin film is due to the effect of electrodes and the structure of the dielectric thin film in a real MIM capacitor.

Bibliography

[1] L. Fang, M. Shen, J. Yang, and Z. Li, Solid State Commun. 137, 381 (2006).

[2] C. Wenger, M. Albert, B. Adolphi, et al., Materials Science in Semiconductor Processing 5, 233 (2003).

[3] M. Ohishi, M. Shiraishi, K. Ochi, Y. Kubozono, and H. Kataura, Appl. Phys Lett. 89, 203505 (2006).

[4] Y. -B. Lin and J. Ya-min Lee, J. Appl. Phys. 87, 1841 (2000).

[5] Neil H. E. Weste and D. Harris, CMOS VLSI Design, A circuit and system perspective, 3rd Edition, (Addison-Wesley, Boston, 2005).

[6] S. M. Sze, Physics of Semiconductor Devices, 2nd ed.,Wiley-Interscience,(1981).

[7] M. Jain, S. B. Majumder, Yu. I. Yuzyuk, R. S. Katiyar, A.S. Bhalla, F.A. Miranda, F.W. Van Keuls, Ferro. Lett. Sectn. 30, 99 (2003).

[8] R. Balachandran, B. H. Ong, H. Y.Wong, K. B. Tan and M. Muhamad Rasat, Int. J. Electrochem. Sci. , 11895 (2012).

[9] N. Y. Chan, G. Y. Gao, Y. Wang, H. L. W. Chan, Thin Solid Films 518, e82 (2010).

[10] M. Jain, S. B. Majumder, R. S. Katiyar, D. C. Agrawal, and A. S. Bhalla, Appl. Phys. Lett. 81, 3212 (2002).

[11] V. Reymond, D. Michau, S. Payan, and M. Maglione, J. Phys. Conden. Matter 16, 9155 (2004).

[12] Jain et al. APL,12,1911(2003).

[13] S. Y. Wang, B. L. CHENG, C. Wang, S.Y. Dai, H. B. Lu, Y. L. Zhou, Z. H. Chen, G. Z. Yang, Appl. Phys. A 81, 1265 (2005).

[14] S. Liu, B. Ma, M. Narayanan, S. Tong, R. E. Koritala, Z. Hu, and U. Balachandran, J. Appl. Phys. 113, 174107 (2013).

[15] T. P. -C. Juan, S. -M. Chen, and J. Y. ?M. Lee, J. Appl. Phys. 95, 3120 (2004).

[16] N. Alimardani, E. W. Cowell, J. F. Wager, J. F. Conley, D. R. Evans, M. Chin, S. J. Kilpatrick, and M. Dubey, J. Vac. Sci. Technol. A 30(1), 01A113-1 (2012).

Dissemination of Work

Conferences

1. **Manjulata Sahoo**, Ratnakar Dash, Banshidhar Majhi, and Santosh K. Sahoo. *Improved Leakage Current of $Ba_{0.8}Sr_{0.2}TiO_3$ Thin Film Capacitors for Dynamic Random Access Memory Applications* accepted at MRS (Materials Research Society) Spring Meeting in San Francisco, California, USA during April 21-25, 2014.